Available online at www.sciencedirect.com
ScienceDirect
Solar Energy 83 (2009) 1588–1598
SOLAR ENERGY
www.elsevier.com/locate/solener

A simple method for quantifying spectral impacts on multi-junction solar cells

G. Peharz *, G. Siefer, A.W. Bett

Fraunhofer-Institut für Solare Energiesysteme, Heidenhofstraße 2, 79110 Freiburg, Germany

Received 7 August 2008; received in revised form 4 May 2009; accepted 20 May 2009
Available online 26 June 2009

Communicated by: Associate Editor Frank Vignola

Abstract

A method to quantify spectral effects on the electric parameters of multi-junction solar cells is presented. The method is based on measuring the short circuit current of at least two monitor cells. Ideally these monitor cells have the same spectral responses as the subcells in the investigated multi-junction solar cell. In contrast to the subcells, the current of the individual monitor cells can be measured separately. This allows conclusions to be drawn about the spectral impact on the current mismatch of the multi-junction solar cell. A spectrometric evaluation method is then applied.

The method has been tested experimentally with three concentrator modules using III–V triple-junction solar cells. These modules were measured outdoors for several months under variable solar spectral conditions. In parallel, the IV curves of the modules and the current of two component cells were measured. A spectral parameter Z was derived from the monitor cell current signals, which was correlated to the short circuit current and the fill factor of the modules. A linear correlation was found between Z and the normalized short circuit current of the concentrator modules. Translation equations were derived from the linear correlation. These enable the calculation of a module's short circuit current under any spectral conditions. In particular, the short circuit currents of the modules were derived for direct normal irradiance of 850 W/m^2 and spectral conditions corresponding to the AM1.5d low AOD spectrum. This is an important step towards comparing the performance of modules which show strong spectral sensitivity. Future rating methods can benefit from the presented simple method for quantifying spectral impacts on multi-junction solar cells. Furthermore, the method can be of interest for tuning the spectrum of pulsed solar simulators.

Keywords: Spectrum; Monitoring; Spectrometric; Rating; PV; Module

1. Introduction

Multi-junction solar cells consist of several subcells with different bandgaps which utilize different parts of the solar spectrum. Consequently, thermalization and transmission losses are reduced and a multi-junction solar cell can convert the solar spectrum more efficiently than a single-junction solar cell. Today, the highest efficiencies are achieved by monolithic III–V triple-junction solar cells (Geisz et al., 2008; Guter et al., 2009; King et al., 2007). The subcells of monolithic multi-junction solar cells are electrically connected in series. Therefore, the short circuit current I_{SC} is determined by the subcell which generates the lowest current. This current limitation is the reason for the pronounced spectral sensitivity of monolithic multi-junction solar cells (Faine et al., 1991; Hein et al., 2001; Kurtz et al., 1990).

Terrestrial applications of III–V multi-junction solar cells are typically in concentrating photovoltaic (CPV) systems (Luque and Andreev, 2007). The characterization of CPV modules equipped with multi-junction solar cell is still challenging. So far, the modules have been measured

* Corresponding author. Tel.: +49 761 4588 5264; fax: +49 761 4588 9250.
E-mail address: gerhard.peharz@ise.fraunhofer.de (G. Peharz).

0038-092X/$ - see front matter © 2009 Elsevier Ltd. All rights reserved.
doi:10.1016/j.solener.2009.05.009

outdoors due to the fact that a quasi-parallel light source on large area is required for indoor measurements. On the other hand, outdoor measurement implies ever changing environmental and spectral conditions. In particular the latter have been not considered so far. Thus, a direct comparison of measurement performed on different modules is difficult. As a result of the combined impact of light concentration and the application multi-junction solar cells, the characterization of CPV modules is still challenging. In this context, one should note that new solar simulators for concentrator modules are currently under development (Anton et al., 2005; Dominguez et al., 2007; Rumyantsev et al., 2006), but these simulators do not allow spectral influences to be investigated. Today a CPV module must be measured outdoors under different solar spectra in order to obtain information about the spectral impact on module performance. Therefore, the solar spectrum must be monitored in parallel to recording the IV curve of the module. In earlier work, the solar spectrum was monitored by using spectroradiometers (Létay et al., 2004; McMahon et al., 2008; Tsutsui and Kurokawa, 2008). A spectroradiometer delivers the complete spectral information, enabling a detailed study of the solar spectrum. Once the spectral distribution is measured the average photon energy can be calculated which is becoming a popular method for quantifying spectral impacts (Krishnan et al., 2009; Minemoto et al., 2009, 2007; van Sark, 2008). One disadvantage of spectroradiometers is that their application is not trivial, especially when outdoor solar spectra are to be measured continuously and reliable over several months. In this paper, an alternative method to monitor the solar spectrum and to quantify its impact on multi-junction solar cells is presented. The measurement technique is based on measuring the current of at least two filtered monitor cells. This makes the method more robust than the application of spectroradiometers. A spectrometric method (Adelhelm and Bücher, 1998; Meusel et al., 2002) is then applied to quantify the spectral impact. This method enables conclusions about the characteristics of the monitored spectrum to be drawn from the measured monitor cell currents. This information can be used to derive the concentrator module performance under given spectral conditions.

2. The spectrometric method

The presented spectrometric method can be applied to investigate spectral influences on the electric properties of multi-junction solar cells. In principle, there are two prerequisites for successful application of the method:

(1) A set of monitor cells with different spectral responses is required. Ideally, the absolute spectral response $SR_i(\lambda)$ of monitor cell i (where λ is the wavelength) is equal to the spectral response of the corresponding subcell in the multi-junction cell. It is recommended to use component cells (also known as "isotype" cells) as monitor cells. The structural composition of component cells is similar to multi-junction cells. In contrast to the multi-junction solar cell, however, the component cell has only one electrically active subcell. Since the other subcells do not have a pn-junction, they are electrically inactive. However, these electrically inactive subcell materials absorb/filter light. Consequently the spectral response of a component cell is expected to be equal to the spectral response of the corresponding subcell in a multi-junction solar cell. An alternative to the use of component cells is the use of single-junction solar cells combined with appropriate bandpass filters.

(2) A defined reference spectrum $E^{ref}(\lambda)$ is required. Whereas flat-plate photovoltaic modules are evaluated using the AM1.5 g spectrum as the standard reference (IEC, 1989), the AM1.5d low AOD (Gueymard et al., 2002) spectrum is often used as the standard for concentrator modules.

The short circuit current density J_{SC} of a solar cell is a function of its spectral response and the irradiance spectrum. With an irradiance spectrum of $E^{ref}(\lambda)$, the short circuit current density J_i^{ref} of monitor cell i is calculated to be:

$$J_i^{ref} = \int SR_i(\lambda) \cdot E^{ref}(\lambda) \cdot d\lambda \quad (1)$$

In a calibration procedure, J_i^{ref} is determined for each monitor cell i. In particular the measurement of the spectral response and a current mismatch correction must be included in the calibration procedure; as described in the IEC standard 60904 Part 7 and 8.

The short circuit current densities of the calibrated monitor cells are measured to monitor the spectra of interest. Each monitor cell i generates a certain short circuit current density J_i^{mon} for the monitored spectrum $E^{mon}(\lambda)$:

$$J_i^{mon} = \int SR_i(\lambda) \cdot E^{mon}(\lambda) \cdot d\lambda \quad (2)$$

The ratio of J_i^{mon} to J_i^{ref} is R_i and describes the current generated under the monitored spectral conditions relative to the current generated with the reference spectrum:

$$R_i = \frac{J_i^{mon}}{J_i^{ref}} = \frac{\int SR_i(\lambda) \cdot E^{mon}(\lambda) \cdot d\lambda}{\int SR_i(\lambda) \cdot E^{ref}(\lambda) \cdot d\lambda} \quad (3)$$

Since the different monitor cells are sensitive to different spectral bands, a conclusion about the spectral distribution of $E^{mon}(\lambda)$ can be drawn by analyzing the current ratios R_i. A spectrometric method (Adelhelm and Bücher, 1998; Meusel et al., 2002) is applied for the analysis. In the following section, this method is described using two monitor cells as an example, and later a more general description is given for an arbitrary number of monitor cells.

2.1. Using two monitor cells

The usage of two monitor cells is recommended to investigate spectral impacts on dual-junction cells. However, it is

also possible to investigate impacts on multi-junction cells with more than two junctions. In particular, two monitor cells are sufficient for the present standard triple-junction cell of $Ga_{0.50}In_{0.50}P/Ga_{0.99}In_{0.01}As/Ge$, because only the top and middle cell are expected to limit the current of the triple cell when it is illuminated with typical solar spectra.

The two monitor cells are illuminated with the spectrum under investigation $E^{mon}(\lambda)$ and their short circuit currents are measured. Subsequently, the ratio of measured and calibrated short circuit currents is determined for the two monitor cells (R_1 and R_2). These are plotted in a two-dimensional plane with two independent axes, r_1 and r_2. This plane is the spectrometric plane illustrated in Fig. 1.

In the spectrometric plane, each point corresponds to one specific pair of current ratios (R_1 and R_2). Since the current ratios contain only integrated spectral information, each pair of current ratios can be generated by an infinite number of spectra. In the spectrometric plane certain lines link spectra which have equal impact on the current generation of the monitor cells:

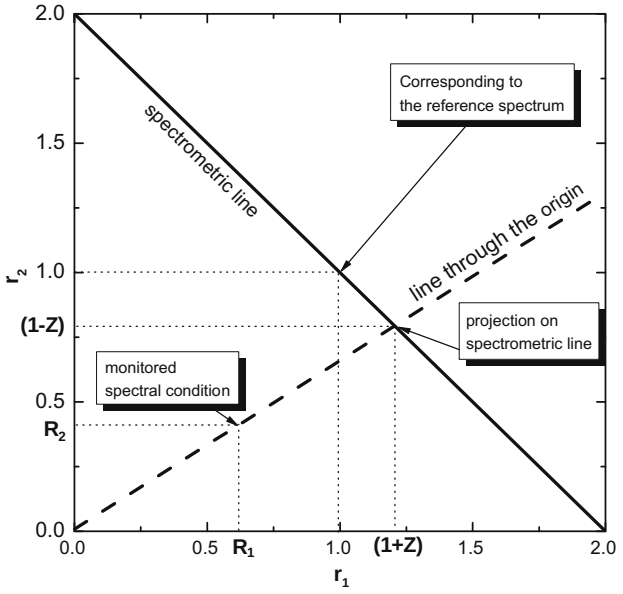

Fig. 1. A spectrometric plane is illustrated. R_1 and R_2 are the monitor cells' monitored currents relative to the calibrated currents determined with the reference spectrum. Each observed spectrum correlates to one point in this plane. However, every point (spectral condition) corresponds to an infinite number of spectra. The point (1;1) corresponds to spectral conditions generating the same absolute currents in both monitor cells as the reference spectrum. Data points located on the same line through the origin have the same relative current ratio R_1/R_2. Thus the relative current generation is the same for all spectra mapped on the same line through the origin. The spectrometric line is defined by $r_1 + r_2 = 2$. This is a line through the point (1;1) and the points (2;0) and (0;2). The latter corresponds to spectral conditions which generate twice the calibrated current in one monitor cell and zero current in the other monitor cell. Every data point on the spectrometric line can be described by a spectral parameter Z.

(1) A line $\frac{r_1}{r_2} = \text{constant}$ defines a line though the origin. All points on the same line through the origin correspond to spectra generating the same current ratio (current mismatch) of monitor cell 1 and monitor cell 2. In particular, the line $r_1 = r_2$ corresponds to spectra which generate the same current mismatch as the reference spectrum does $\left(\frac{J_1^{mon}}{J_2^{mon}} = \frac{J_1^{ref}}{J_2^{ref}}\right)$. Spectra which generate $\frac{J_1^{mon}}{J_2^{mon}} < \frac{J_1^{ref}}{J_2^{ref}}$ are mapped in the area above the line $r_1 = r_2$. Other spectra which generate relatively more current in monitor cell 1 are related to points below this line.

(2) In contrast to lines through the origin, lines defined by $r_1 + r_2 = \text{constant}$ correspond to spectra which generate the same absolute total current mismatch. However, different points on these lines are related to different current mismatches. In particular the spectrometric line ($r_1 + r_2 = 2$) is of interest. This line passes through the points (1;1), (0;2) and (2;0). The point (1;1) corresponds to spectra which generate the same absolute currents in each of the monitor cells as the reference spectrum does. The point (0;2) corresponds to spectra which generate twice the calibrated current in monitor cell 2 and zero current in monitor cell 1. Conversely, monitor cell 1 generates twice the calibrated current and monitor cell 2 generates zero current for spectra mapped to (2;0). Beside these two extreme cases, every other intermediate current mismatch can be found on the spectrometric line.

The current mismatch of different points on the spectrometric line defined above can be expressed by a single parameter Z (Adelhelm and Bücher, 1998; Meusel et al., 2002):

$$R_1 - 1 = Z = 1 - R_2 \tag{4}$$

In order to determine Z for all other points in the spectrometric plane, they are projected by a line through the origin onto the spectrometric line. The projection of an arbitrary point onto the spectrometric line is illustrated in Fig. 1. This projection normalizes the absolute total current mismatch of the two monitor cells to the absolute current for the reference spectrum (x indicates the initial values and y indicates the projected values):

$$R_1^y = \frac{2^* R_1^x}{R_1^x + R_2^x} \tag{5}$$

$$R_2^y = \frac{2^* R_2^x}{R_1^x + R_2^x} \tag{6}$$

Consequently, a spectral parameter Z can be determined for each monitored spectrum. Z describes the current mismatch relative to the current mismatch for the reference spectrum. Since the spectral responses of the monitor cells and the subcells are almost identical, the current mismatch in the investigated dual-junction cell is similar. Please note that in reality the spectral responses will not be perfectly identical. This minor mismatch of the spectral responses

is considered to be the main error source of the presented method. However, a detailed error analysis would require more finely resolved spectral information, for example from measuring the spectrum $E^{mon}(\lambda)$ with a spectroradiometer in parallel. In this work no measurements with a spectroradiometer were performed. This will be part of further investigations.

The spectrometric plane is primarily useful to illustrate the impact of an arbitrary spectrum on the current generation of the monitor cells and to derive the spectral parameter Z, which in turn can be correlated to the performance of a dual-junction cell under varying spectral conditions. When more than two monitor cells are used, the mathematical procedure is the same in principle. However, the representation becomes multi-dimensional.

2.2. Using more than two monitor cells

When the spectral impact is determined with more than two monitor cells, in principle the same procedure can be applied and the current ratios R_i are determined for each monitor cell i, as described in Eq. (1).

The monitored spectra are characterized by a set of N different ratios R_i, where N is the total number of monitor cells. Each spectral condition is represented as a data point in an N-dimensional space with different independent current ratios R_i. The spectrometric function is defined as follows:

$$\sum_{i=1}^{N} r_i = N \tag{7}$$

For normalization, each data point is projected onto the spectrometric function by applying the following equation:

$$\mathrm{R}'_i = \frac{N}{\sum_{i=1}^{N} R_I} \cdot R_i \tag{8}$$

where R'_i is the projected current ratio of the original value R_i. The projected value of the current ratio provides normalized information about the current mismatch relative to the current mismatch for the reference spectrum.

The analysis of the current mismatch is more challenging for a multi-dimensional spectrometric function. Algebraic simplifications are necessary to draw illustrative conclusions. However, this is a topic of further research and is not addressed in this paper.

3. Experimental

The presented method for quantifying spectral impacts was experimentally tested for concentrator PV (CPV) modules. In particular, the impact of the solar spectrum on the current generation and the fill factor of these modules was investigated. Three different CPV modules using III–V triple-junction solar cells were investigated. Module #1 was manufactured by Daido Steel (Araki, 2007; Araki et al., 2005) and modules #2 and #3 were FLATCON® type modules (Bett et al., 2005; Bett and Lerchenmueller, 2007). All three modules were equipped with $Ga_{0.50}In_{0.50}P/Ga_{0.99}In_{0.01}As/Ge$ triple-junction solar cells. However, the thickness of the top cells ($Ga_{0.50}In_{0.50}P$) was different. The cells in module #1 are optimized for the AM1.5 g spectrum (IEC, 1989), the cells in module #2 are optimized for the AM0 spectrum (ISO, 2005) and the cells in module #3 are optimized for the AM1.5d low AOD spectrum (Gueymard et al., 2002). Table 1 summarizes the main features of the different modules. Furthermore the measured external quantum efficiency of a typical $Ga_{0.50}In_{0.50}P/Ga_{0.99}In_{0.01}As/Ge$ triple-junction optimized for the AM1.5d low AOD spectrum is shown in Fig. 2. Please note, that the quantum efficiency of a CPV module is also impacted by the concentrating optics and the increased cell temperature.

It must be pointed out that for terrestrial spectra, the germanium bottom cell in a $Ga_{0.50}In_{0.50}P/Ga_{0.99}In_{0.01}As/Ge$ triple-junction cell typically generates 30–50% more current than the $Ga_{0.50}In_{0.50}P$ top cell or the $Ga_{0.99}In_{0.01}As$ middle cell. Consequently, the germanium bottom cell is not expected to limit the current. Therefore, two monitor cells are sufficient. The tests were performed outdoors on the roof of Fraunhofer ISE (latitude 48.01° north and longitude 7.83° east). A measurement stand for CPV modules is installed, which measures IV curves of up to 20 concentrator modules automatically (Siefer and Bett, 2005, 2004). In addition, the direct normal irradiance DNI is measured with an Eppley NIP pyrheliometer (opening angle = ±2.9°) and the global normal irradiance GNI is measured with an ESTI sensor (Ossenbrink and Münzer, 1992). The accuracy

Table 1
Three different CPV modules were monitored under varying outdoor spectral conditions. Lattice-matched triple-junction solar cells optimized for different spectra operate in the modules. The measurement period, the type of module and the type of solar cells used are shown. Furthermore, the number of evaluated measurements (after data filtering) is indicated. Please note that module #2 was not measured during the period from July to September 2008, due to a broken support. The angular acceptance angle of module #1 is about ±1° and the other two modules have an acceptance angle of about ±0.5°. Please note, that there is no established rating procedure for CPV modules at the moment. Consequently it is not possible to provide rated module efficiencies. However, typically the outdoor measured efficiency of these modules ranges between 20 and 26%.

Module #	Type	Solar cells	Measurement period	Number of measurements
1	Daido Steel	Triple-junction (AM1.5 g)	October 2007–November 2008	11434
2	FLATCON®	Triple-junction (AM0)	October 2007–June 2008 October 2008–November 2008	5577
3	FLATCON®	Triple-junction (AM1.5d low AOD)	May 2008–November 2008	7491

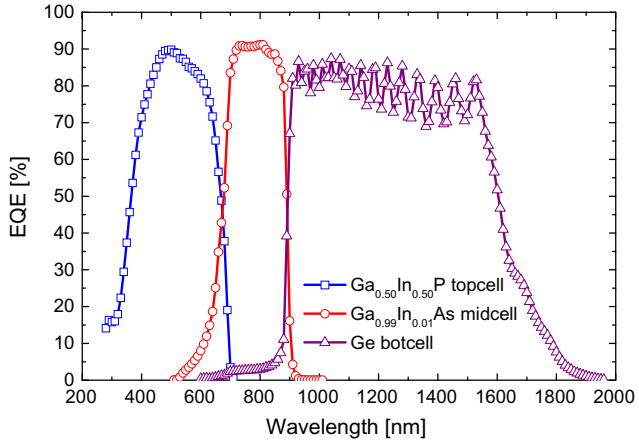

Fig. 2. The external quantum efficiency of a typical $Ga_{0.50}In_{0.50}P$/$Ga_{0.99}In_{0.01}As$/Ge triple-junction cell is shown. The measurements were performed for each subcell separately and were taken at a cell temperature of 25 °C.

of both irradiation measurement instruments should be better than 5%.

Two encapsulated component cells were used for the spectral monitoring. The external quantum efficiencies of these cells are plotted in Fig. 3. The first cell is a $Ga_{0.50}In_{0.50}P$ cell, which is the same as the top cell in the lattice-matched triple-junction solar cell used in the CPV modules. Secondly, a $Ga_{0.83}In_{0.17}As$ component (middle) cell is used, which receives light filtered by the electrically inactive $Ga_{0.35}In_{0.65}P$ material. The second monitor cell is sensitive to wavelengths between 680 and 1050 nm. It should be noted that this monitor cell has a broader spectral response than the middle cells used in the CPV modules. The middle cells in the modules are sensitive to wavelengths between 680 and 890 nm. Consequently, the spectral response of this monitor cell is not equal to the spectral response of the corresponding subcell. This non-ideal monitor cell was used only for availability reasons. The relative variation of the current mismatch with changing solar spectra is expected to be similar for the monitor cells and the triple-junction cells in the modules. However, for certain solar spectra the absolute current mismatch can be estimated to be different in the range of several percent.

The encapsulated component cells were calibrated at the ISE CalLab and their calibrated short circuit currents I_{SC} were determined for the reference spectrum AM1.5d low AOD (Gueymard et al., 2002) ($G = 1000\ W/m^2$).

In October 2007, the monitor cells were mounted onto the outdoor measurement stand. The monitor cells are located behind collimator tubes, providing an opening angle of ±2.5°. A photograph of the outdoor test stand is shown in Fig. 4.

The IV curve of the modules and the DNI were measured. In order to take the DNI value into account, which represents the major influence on the module's short circuit current I_{SC}, the intensity was (linearly) normalized to 850 W/m^2:

$$\text{normalized } I_{SC}[\text{mA}] = \frac{\text{measured } I_{SC}[\text{mA}] \cdot 850\ \text{W/m}^2}{\text{measured DNI } [\text{W/m}^2]} \tag{9}$$

The DNI level of 850 W/m^2 was chosen because it is a typical used as a reference condition for concentrator applications (ASTM, 2006). The short circuit current of the monitor cells I_i^{mon} is monitored in parallel to each module IV curve. The time base of the monitoring was in the range of minutes. Since their short circuit currents I_i^{ref} are known for the reference spectrum, the spectral parameter Z can be determined for every module IV curve measurement (see Section 2).

The spectral responses of the subcells in the investigated modules and the spectral response of the monitor cells are similar but not identical. Consequently the current mismatches generated are not expected to be absolutely identical. However, it is assumed that the current mismatch of the triple-junction cells is linearly dependent on the current

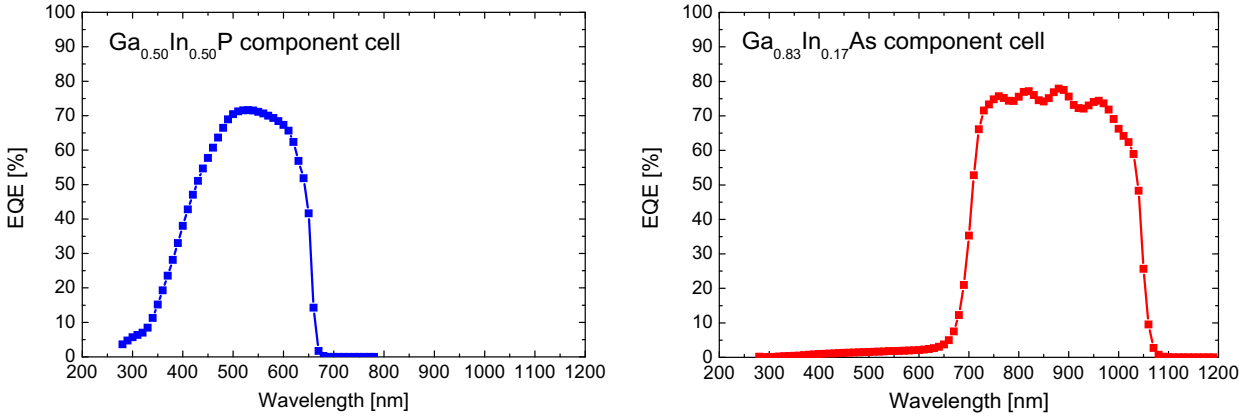

Fig. 3. The external quantum efficiency of the two component cells used as monitor cells for the present study: On the left, the external quantum efficiency of the encapsulated top monitor cell is shown. On the right, the same quantity is shown for the encapsulated middle monitor cell. The latter is filtered by the electrically inactive $Ga_{0.35}In_{0.65}P$ top-cell material. The measurements were taken at a cell temperature of 25 °C.

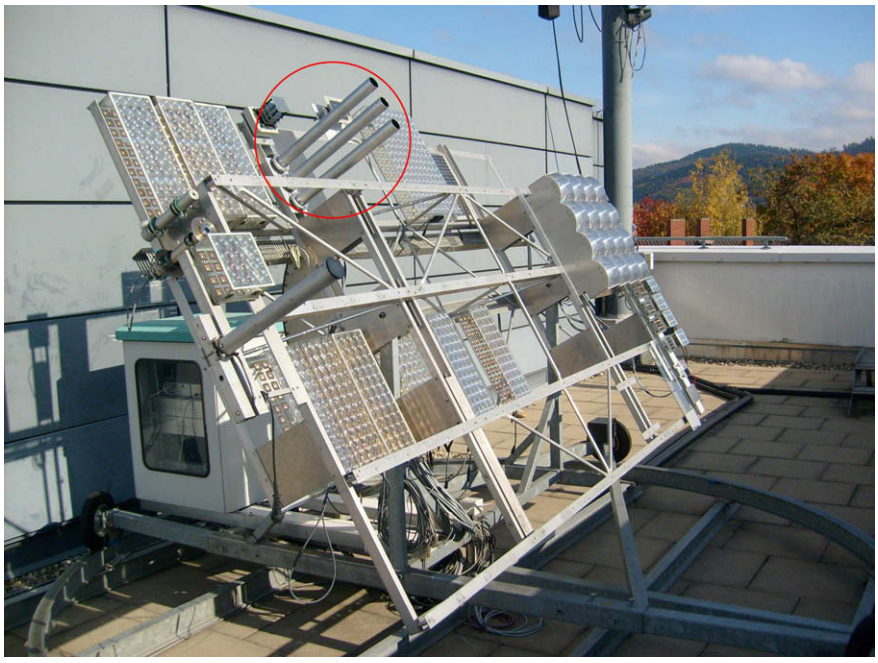

Fig. 4. A photograph of the outdoor test stand for characterizing CPV modules is shown. One can see clearly the two axis tracking system with several mounted modules. In October 2007, filtered monitor cells were mounted behind collimator tubes, in order to monitor the spectral conditions of the direct irradiance. The position of three collimator tubes is marked. The monitor cells used for the present study are located behind two of them.

mismatch of the monitor cells (expressed by Z). Beside the current mismatch of the subcells the module's I_{SC} is impacted by the tracking accuracy, the circum solar radiation and the cell temperature. Furthermore dust and dew on the optics and/or the pyrheliometer can influence the normalized I_{SC}.

The spectral impact on the fill factor must also be discussed, taking the complete IV curve of the module into account. The spectral impact on the fill factor of a multijunction solar cell was investigated in earlier papers (Adelhelm and Bücher, 1998; Meusel et al., 2002). There it was found that at one sun the magnitude of the current mismatch effect on the fill factor was about three times lower than the effect on the short circuit current. Further impact factors on the modules fill factor are the temperature, the DNI, the tracking accuracy and also the circum solar radiation. Additionally dust and dew also can influence the fill factor of the modules.

The value $Z = 0$ corresponds to spectral conditions which generate the same (relative) current mismatch in the monitor cells as the AM1.5 low AOD reference spectrum (Gueymard et al., 2002). Z values < 0 correspond to spectra which generate relatively more current in the middle monitor cell. Consequently these spectra are "red-richer" than the reference spectrum. By contrast, Z values > 0 correspond to spectra, which are more "blue-rich" than the reference spectrum.

Finally, it should be noted that neither the IV curves of the modules nor the short circuit currents of the monitor cells were temperature-corrected. It is expected that the cells in the modules operated at higher temperatures. The solar cell temperature is difficult to measure in concentrator photovoltaic modules, however the absolute temperature difference to the monitor cells is expected to be <10 K. Please note, that an increased temperature causes a shift in the band edge of the cells and increases the short circuit current. Typically the short circuit current temperature coefficient of III–V solar cells is in the range of 0.05–0.09%/K (Siefer et al., 2005). Thus the impact of the cell temperature on the analysis can expected to be <1%.

4. Results

The IV curves of the CPV modules were measured whenever the DNI was >100 W/m^2. The parameters fill factor, efficiency and the ratio DNI/GNI, were used for data filtering. About 20% of the data was excluded by applying the filtering procedures described below.

A low measured efficiency (<10%) indicates that either the module was not well aligned or condensation on the lenses had decreased the efficiency. IV curves with a comparatively low fill factor (<70%) indicate that the module was not well aligned during the measurement (due to tracking errors).

The triple-junction cells used in the modules typically show maximum fill factors of 90% and efficiencies of 35% when measured indoors under varying spectral conditions (Meusel et al., 2006). The module efficiency is mainly determined by the efficiency of the solar cells, optical losses and temperature effects. Consequently, module fill factors >90% and module efficiencies >30% are assumed to be unrealistically high values for the investigated modules

(all cells are protected with bypass diodes). Please note that unrealistic high fill factors are usually caused by a varying DNI or a tracking error during the IV measurement, which typically takes 10 s. Furthermore an unrealistic high efficiency is mostly related to a partly shadowed pyrheliometer. Therefore, the analysis considered only module IV curves satisfying the two conditions, 70% < fill factor < 90% and 10% < efficiency < 30%.

Another sorting criterion for the analysis was the requirement to have DNI/GNI ratios >0.75. This was motivated by the possible impact of the circumsolar radiation (CSR) on the current of a CPV module. The CSR is caused by forward scattering of light on passing through the atmosphere. Observed from the ground, the CSR is visible as an enlargement of the solar disc. In contrast the investigated concentrator modules have a smaller acceptance angle than that of the pyrheliometer (±2.9°). Under conditions with a relatively high CSR, the pyrheliometer measures a significantly higher DNI than can be utilized by the CPV modules. Consequently, under conditions with a high CSR, the current of the modules is lower than under low CSR conditions. High CSR conditions are expected to correlate to a hazy sky and DNI/GNI ratios <0.75. Please note, that no correlation was found between the DNI/GNI ratio and the observed spectral condition Z. Consequently, the filtering of hazy conditions is not expected to have a significant impact on the spectral analysis.

4.1. Module #1

Fig. 5 shows the normalized I_{SC} of module #1 versus the spectral parameter Z. The normalized I_{SC} of module #1 increases linearly with the spectral parameter up to a value of $Z \cong 0.03$. At this value of Z, the normalized I_{SC} reaches a local maximum. The normalized I_{SC} decreases again for spectral parameters $Z > 0.03$. It is concluded that under spectral conditions which correspond to $Z \cong 0.03$, the triple-junction solar cells in the module operate in the current-matched mode. This seems reasonable, because the cells in module #1 are optimized for the AM1.5 g spectrum (IEC, 1989) which is slightly richer in the blue spectral range than the AM1.5d low AOD reference spectrum (Gueymard et al., 2002). For Z values > 0.03, the middle cells are expected to become the limiting subcells in the module and for Z values < 0.03 the top cells limit the current.

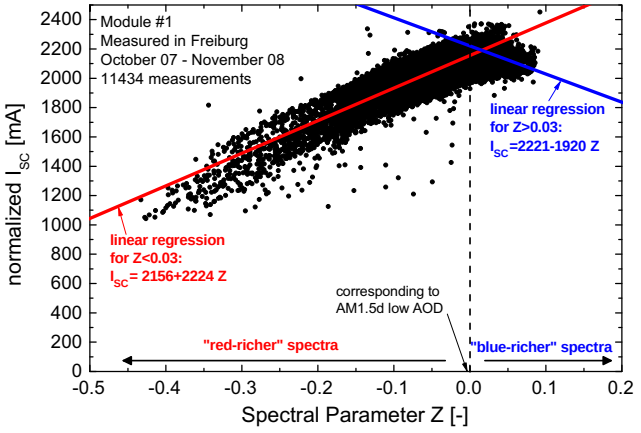

Fig. 5. Module #1: normalized I_{SC} versus spectral parameter Z. Between October 2007 and November 2008, a total number of 11434 measurements was evaluated. The normalized I_{SC} reaches a maximum at $Z \cong 0.03$. Linear regressions were performed separately for data with $Z < 0.03$ resulting in a function: $I_{SC} = 2156\ (\pm 1) + 2224\ (\pm 12)\ Z$ ($R^2 = 0.77$) and $Z > 0.03$ resulting in a function: $I_{SC} = 2221\ (\pm 5) + 1920\ (\pm 108)\ Z$ ($R^2 = 0.15$). Please note that a linear regression over the total range of Z results in a R^2 of 0.84 and a slope of 1930 (±12). Consequently the relative slope error is slightly better when fitting the data with $Z < 0.03$ than fitting the total range of data. The triple-junction cells in this module are optimized for the AM1.5 g reference spectrum.

A linear regression of all data with $Z < 0.03$ delivers the function: normalized $I_{SC}[\text{mA}] = 2156\ \text{mA} + 2224\ \text{mA} \cdot Z$; a fit for $Z > 0.03$ delivers the function normalized $I_{SC}[\text{mA}] = 2221\ \text{mA} - 1920\ \text{mA} \cdot Z$. These linear correlations directly deliver the spectral sensitivity of the module's I_{SC}. Consequently, translation equations can be defined which describe the relative impact of Z on the I_{SC} of module #1. When the I_{SC} is known for a certain value of $Z \rightarrow I_{SC}(Z_1)$, the I_{SC} can be determined for any other value of $Z \rightarrow I_{SC}(Z_2)$:

$$I_{SC}(Z_2)[\text{mA}] = I_{SC}(Z_1)[\text{mA}] + 2224\ \text{mA} \cdot (Z_2 - Z_1) \quad (Z \leqslant 0.03) \tag{10}$$

$$I_{SC}(Z_2)[\text{mA}] = I_{SC}(Z_1)[\text{mA}] - 1920\ \text{mA} \cdot (Z_2 - Z1) \quad (Z \geqslant 0.03) \tag{11}$$

The translation equations 8 and 9 are defined differently for the two separate value ranges of Z ($Z \leqslant 0.03$ and $Z \geqslant 0.03$). Translations between these two different ranges can be made by calculating the intermediate result of $I_{SC}(Z = 0.03)$. The translation equations can be applied to calculate the normalized I_{SC} for a certain spectral parameter Z.

In particular, each normalized I_{SC} shown in Fig. 5 is translated to $Z = 0$. By applying the normalization and the translation to $Z = 0$, the I_{SC} of module #1 is determined for a DNI of 850 W/m^2 at spectral conditions corresponding to the AM1.5d low AOD spectrum (Gueymard et al., 2002). Consequently the influence of the DNI and the impact of the spectrum are ruled out. In Table 2, the mean value and the standard deviation of the I_{SC} are documented for module #1. Furthermore, the same statistical parameters are shown for the normalized I_{SC}, and for the normalized I_{SC} translated to $Z = 0$.

Obviously the standard deviation decreases when the influence of the DNI is eliminated. The standard deviation is further reduced by excluding the impact of the solar spectrum. The final standard deviation is reduced to 4.5% of the mean value. This is remarkably low, considering that this is based on more than 11,000 IV curve measurements taken outdoors over a period of more than a year. Please

Table 2
The mean value and the standard deviation of the I_{SC} measured for module #1 are listed. Furthermore the same statistical parameters are given for the normalized I_{SC}, and for the normalized I_{SC} translated to $Z = 0$. The number of evaluated measurements is 11434.

	I_{SC}	I_{SC} normalized (850 W/m^2)	I_{SC} normalized (850 W/m^2) and translated to $Z = 0$
Mean (mA)	1761	2041	2141
Standard deviation (mA)	387	186	97
$\frac{\text{standard deviation}}{\text{mean}} \cdot 100\%$ (%)	22	9.1	4.5

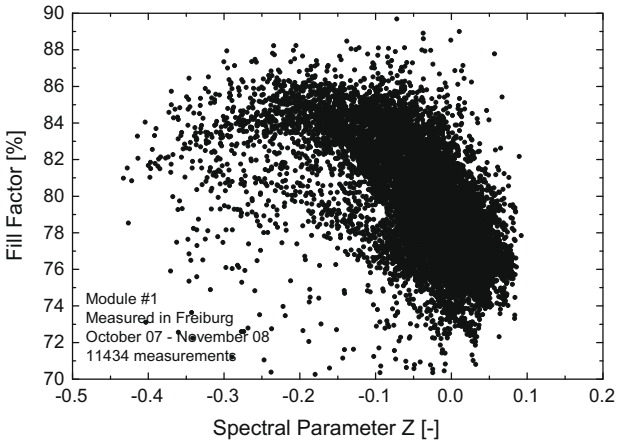

Fig. 6. The fill factor of module #1 is plotted versus the spectral parameter Z. A trend toward decreasing fill factors is observed for increasing Z. However, there is a large variance in the data. Most probably other factors (e.g. module temperature, CSR and tracking errors) influence the modules' fill factor by a similar amount to the spectrum.

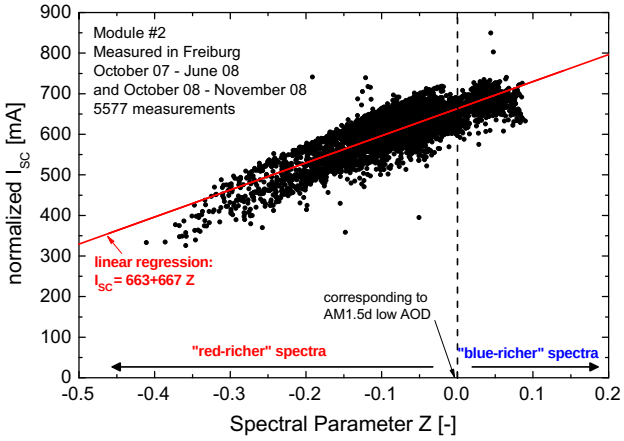

Fig. 7. Module #2: normalized I_{SC} versus spectral parameter Z. The total number of evaluated measurements is 5577. In the period between July and September 2008, the module support was broken and no measurements were taken. A linear regression results in the function: $I_{SC} = 663\ (\pm 0.6) + 667\ (\pm 5.7)$ ($R^2 = 0.71$). The triple-junction cells in this module are optimized for the AM0 reference spectrum (ISO, 2005). Obviously there is no current matching observed for this module. The normalized I_{SC} increases linearly with the spectral parameter Z.

note that these measurements include temperature effects and still some CSR variation and tracking errors.

In Fig. 6, the fill factor of module #1 is plotted versus the spectral parameter. The fill factor decreases for increasing Z. However, the variance of the data is relatively high and no clear functional dependence was found. Apparently other factors influence the fill factor to a similar extent as the spectrum. These other factors could be the module temperature, CSR, tracking errors and the DNI. Additionally dust and dew on the modules can impact the fill factor.

4.2. Module #2

Fig. 7 shows the normalized I_{SC} of module #2 versus the spectral parameter Z. The normalized I_{SC} increases continuously for all observed spectral conditions. Current matching was not observed for this module. This is not surprising, because the cells in the module are optimized for the very blue-rich AM0 spectrum (ISO, 2005) and such spectral conditions are not expected in geographical locations such as Freiburg.

When the data of module #2 are fitted, the linear function $\text{normalized } I_{SC}[\text{mA}] = 663\ \text{mA} + 667\ \text{mA} \cdot Z$ is obtained. From the gradient, a translation equation can be obtained, which describes the translation of $I_{SC}(Z_1)$ to $I_{SC}(Z_2)$:

$$I_{SC}(Z_2)[\text{mA}] = I_{SC}(Z_1)[\text{mA}] + 667\ \text{mA} \cdot (Z_2 - Z_1) \qquad (12)$$

All normalized I_{SC} values of module #2 are translated to $Z = 0$. Table 3 shows the mean values and the standard deviation of the I_{SC}, the normalized I_{SC} and the normalized I_{SC} translated to $Z = 0$.

The standard deviation of the I_{SC} is significantly reduced by applying the normalization and the translation to $Z = 0$. The remaining standard deviation is most probably caused by other impacts (e.g. temperature, CSR, tracking errors).

Fig. 8 shows the fill factor of module #2 versus the spectral parameter Z. The fill factor appears to decrease with increasing Z. However, the functional trend is not clear. Perhaps the fill factor of this module is more influenced by other factors than by the solar spectrum.

4.3. Module #3

Fig. 9 shows the normalized I_{SC} of module #3 versus the spectral parameter Z. The maximum normalized current of this module is observed at $Z \cong 0.0$. This is reasonable, because this module uses triple-junction solar cells which are designed to be current-matched for the AM1.5d low AOD spectrum (Gueymard et al., 2002). For spectral conditions with $Z < 0.0$, obviously the top cell in the module

Table 3
The mean value and the standard deviation of the I_{SC} measured for module #2 are shown. Furthermore, the same statistical parameters are listed for the normalized I_{SC}, and the normalized I_{SC} translated to $Z = 0$. The number of evaluated measurements is 5577.

	I_{SC}	I_{SC} normalized (850 W/m^2)	I_{SC} normalized (850 W/m^2) and translated to $Z = 0$
Mean (mA)	518	618	663
Standard deviation (mA)	125	63	34
$\frac{\text{standard deviation}}{\text{mean}} \cdot 100\%$ (%)	24	10.2	5.1

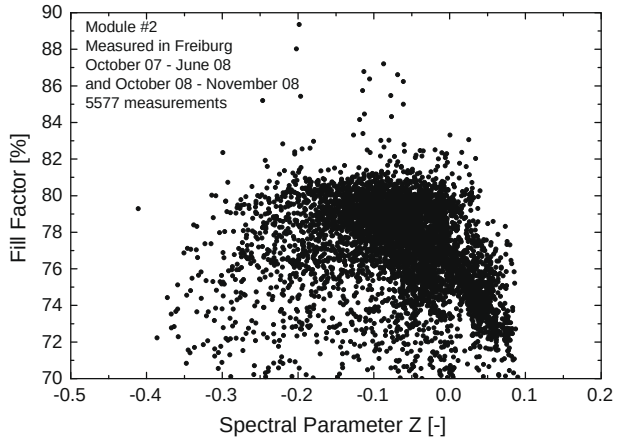

Fig. 8. The fill factor of module #2 is plotted versus the spectral parameter Z. A trend toward decreasing fill factors is observed for increasing Z. However, there is a large variance in the data. Most probably other factors (e.g. module temperature, CSR and tracking errors) influence the modules' fill factor by a similar amount to the spectrum.

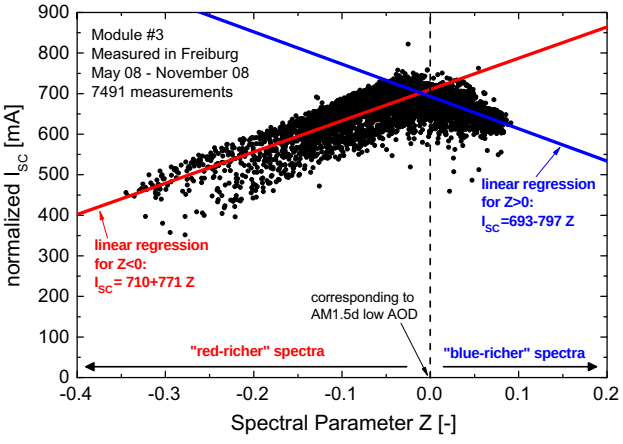

Fig. 9. Module #3: normalized I_{SC} versus spectral parameter Z. Between May 2008 and November 2008 a total number of 7491 measurements was recorded. The normalized I_{SC} reaches a maximum at $Z \cong 0.0$. Accordingly, the cells in the module are current-matched at Z values around zero. Two linear regressions were performed for data with $Z < 0.0$ and $Z > 0.0$. The resulting functions are $I_{SC} = 710\ (\pm 0.8) + 771\ (\pm 8.5)\ Z$ ($R^2 = 0.65$) and $I_{SC} = 693\ (\pm 0.7) + 797\ (\pm 21.1)\ Z$ ($R^2 = 0.31$). The triple-junction cells in this module are optimized for the AM1.5d low AOD spectrum (Gueymard et al., 2002).

limits the current and for $Z > 0.0$, the middle cell limits the current.

A linear regression for the data with $Z < 0$ delivers the function: $\text{normalized } I_{SC}[\text{mA}] = 710\ \text{mA} + 771\ \text{mA} \cdot Z$. The function $\text{normalized } I_{SC}[\text{mA}] = 693\ \text{mA} - 797\ \text{mA} \cdot Z$ is obtained for data with $Z > 0$. The translation equations for calculating the normalized short circuit current for any spectral parameter Z are derived from the linear regressions:

$$I_{SC}(Z_2)[\text{mA}] = I_{SC}(Z_1)[\text{mA}] + 771\ \text{mA} \cdot (Z_2 - Z_1) \quad (Z \leqslant 0) \tag{13}$$

$$I_{SC}(Z_2)[\text{mA}] = I_{SC}(Z_1)[\text{mA}] - 797\ \text{mA} \cdot (Z_2 - Z_1) \quad (Z \geqslant 0) \tag{14}$$

The normalized I_{SC} values of module #3 are translated to $Z = 0$. Consequently the spectral impact and the impact of the DNI on the modules's I_{SC} are excluded. In Table 4, the mean value and the standard deviation are listed for the I_{SC}, the I_{SC} normalized to 850 W/m^2 and the normalized I_{SC} translated to $Z = 0$.

As shown in Fig. 9, this module is current-matched at Z values around zero. The number of top-cell limitations and middle-cell limitations is better balanced than for the other two modules. However, the spectral impact on module #3 is still obvious. By normalizing the measured I_{SC} and translating the normalized I_{SC} to $Z = 0$, the relative standard deviation is reduced from 18.6% to 7.2% and 4.4%, respectively.

No clear correlation is found between the fill factor and the spectral parameter Z for module #3, as indicated by the plot in Fig. 10. Apparently the fill factor decreases for an increasing spectral parameter Z until $Z \cong 0$. For higher values of Z, the fill factor seems to increase. However, the data is too noisy to draw a clear conclusion.

5. Conclusion

In this paper, a method has been presented for quantifying spectral impacts on multi-junction solar cells applied in concentrator photovoltaic (CPV) modules. Three different modules were investigated outdoors over several months under varying solar spectral conditions. A linear correlation was found between the spectral parameter Z and the short circuit current of the modules. Furthermore, the spectral conditions for current matching were identified for two modules. Translation equations were derived from the linear correlations which enable the module's short circuit current to be calculated for any spectral conditions. In particular, the modules' short circuit currents were calculated with respect to a direct normal irradiance of 850 W/m^2 and spectral conditions corresponding to the AM1.5d low AOD spectrum.

Table 4
The mean value and the standard deviation of the I_{SC} measured for module #3 are listed. Furthermore the same statistical parameters are given for the normalized I_{SC}, and the normalized I_{SC} translated to $Z = 0$. The number of evaluated measurements is 7491.

	I_{SC}	I_{SC} normalized (850 W/m^2)	I_{SC} normalized (850 W/m^2) and translated to $Z = 0$
Mean (mA)	580	662	703
Standard deviation (mA)	108	48	31
$\frac{\text{standard deviation}}{\text{mean}} \cdot 100\%$ (%)	18.6	7.2	4.4

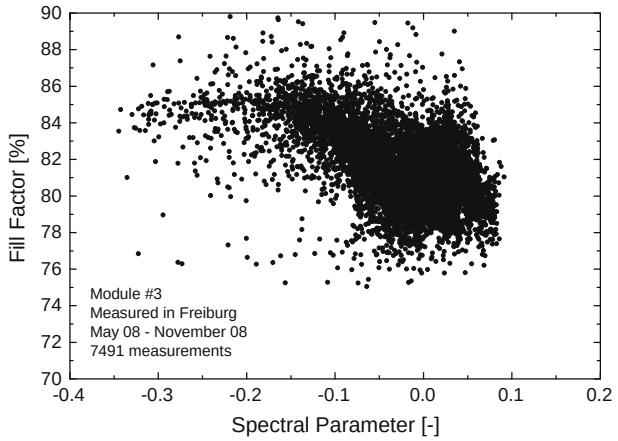

Fig. 10. The fill factor of module #3 is plotted versus the spectral parameter Z. A trend toward decreasing fill factor is observed for increasing Z. The FF may increase slightly for $Z > 0$. However, the data shows a too large variance to draw a clear conclusion. Most probably other factors (e.g. module temperature, CSR and tracking errors) influence the module's fill factor to a similar extent to the spectrum.

From the experimental results, it can be concluded that the presented method works at least for the outdoor characterization of CPV modules equipped with triple-junction cells. A second important conclusion is that this method is quite robust. Although monitor cells were used which were not ideally matched to the spectral responses of the investigated subcells, the proposed method functioned sufficiently well to quantify the spectral influence on the CPV module performance. A weak point of the method is that the accuracy is limited. For more exact studies of the spectral impact on CPV modules, an accurate spectroradiometer should be used.

It is recommended to use the presented method for long-term outdoor investigations of CPV modules and systems. Usually, many uncontrolled factors influence the data points measured outdoors. Thus, it is advantageous to apply the more robust and simpler method and accept the lower accuracy. In the present study, the accuracy of the method has not been fully analyzed. The monitored spectrum must be known exactly to calculate the accuracy of the presented method in more detail. However, when the standard deviation of the presented results is considered, the accuracy is estimated to be on the order of a few percent.

From earlier work at the cell level (Adelhelm and Bücher, 1998; Meusel et al., 2002), a spectral impact on the module fill factor can also be expected. In the presented results at the module level, no clear correlation was found between the module fill factor and the spectral parameter Z. It is concluded that the spectral impact on the fill factor of CPV modules is of a similar magnitude to other factors. For instance the module temperature, the circumsolar radiation, the direct normal irradiation and especially tracking errors also affect the fill factor of CPV modules.

One application of the method can be in the development of rating procedures for spectrally sensitive CPV modules. The impact of varying solar spectra on a CPV module equipped with multi-junction cells can be quantified. Finally, the short circuit current of the module can be identified with respect to a certain reference spectrum and a reference direct normal irradiance value. Despite the fact that the method was tested only with CPV modules with III–V multi-junction cells, it should be applicable to other multi-junction technologies (e.g. thin film multi-junction cells and modules). However, this must be tested in future work.

Beside applications to outdoor measurements, the presented method can be used to tune pulsed solar simulators. The measurement of a pulsed simulator spectrum is very challenging. By contrast, the measurement of a current signal is much simpler. With an appropriate set of monitor cells, the pulsed simulator spectrum can be quantified simply and quickly. Once the spectrum can be quantified, the effect of tuning can be monitored.

Acknowledgments

The authors gratefully acknowledge Kenji Araki for providing the Daido Steel module and information. Furthermore the authors would like to thank Armin Bösch, Raymond Hoheisel and Helen Rose Wilson for their support. This work has been partly supported by the German Federal Ministry for the Environment, Nature Conservation and Nuclear Safety (BMU) under the ProKonPV project (contract 0327567). The authors are responsible for the content of this paper.

References

Adelhelm, R., Bücher, K., 1998. Performance and parameter analysis of tandem solar cells using measurements at multiple spectral conditions. Solar Energy Materials and Solar Cells 50, 185–195.

Anton, I., Dominguez, C., Sala, G., Martinez, M., Diaz, V., Alvarez, J.L., Alonso, J., 2005. Indoor characterization of concentrator modules: application on the production line. In: Proceedings of the 3rd

International Conference on Solar Concentrators for the Generation of Electricity or Hydrogen, NREL-CD 520-38172.

Araki, K., 2007. 500X to 1000X – R&D and market strategy of daido steel. In: Proceedings of the 4th International Conference on Solar Concentrators for the Generation of Electricity or Hydrogen, pp. 73–76.

Araki, K., Uozumi, H., Egami, T., Hiramatsu, M., Miyazaki, Y., Kemmoku, Y., Akisawa, A., Ekins Daukes, N.J., Lee, H.S., Yamaguchi, M., 2005. Development of concentrator modules with dome-shaped Fresnel lenses and triple-junction concentrator cells. Progress in Photovoltaics: Research and Applications 13, 513–527.

ASTM E 2527–06, Standard Test Method for Rating Electrical Performance of Concentrator Terrestrial Photovoltaic Modules and Systems Under Natural Sunlight, 2006.

Bett, A.W., Baur, C., Dimroth, F., Lerchenmueller, H., Siefer, G., Willeke, G., 2005. The FLATCON® concentrator PV-technology. In: Proceedings of the 3rd International Conference on Solar Concentrators for the Generation of Electricity or Hydrogen, NREL-CD 520-38172.

Bett, A.W., Lerchenmueller, H., 2007. The FLATCON® system from concentrix solar. Concentrator Photovoltaics. Springer-Verlag GmbH, pp. 301–319.

Dominguez, C., Anton, I., Sala, M. Ballack, G., Martinez, M., 2007. Description and validity assesment of a solar simulator for high concentration PV modules. In: 22nd European Photovoltaic Solar Energy Conference, pp. 136–139.

Faine, P., Kurtz, S.R., Riordan, C., Olson, J.M., 1991. The influence of spectral solar irradiance variations on the performance of selected single-junction and multijunction solar cells. Solar Cells 31, 259–278.

Geisz, J.F., Friedman, D.J., Ward, J.S., Duda, A., Olavarria, W.J., Moriarty, T.E., Kiehl, J.T., Romero, M.J., Norman, A.G., Jones, K.M., 2008. 40.8% efficient inverted triple-junction solar cell with two independently metamorphic junctions. Applied Physics Letters 93, 123505/1–123505/3.

Gueymard, C.A., Myers, D., Emery, K., 2002. Proposed reference irradiance spectra for solar energy systems testing. Solar Energy 73, 443–467.

Guter, W., Schöne, J., Philipps, S.P., Steiner, M., Siefer, G., Wekkeli, A., Welser, E., Oliva, E., Bett, A.W., Dimroth, F., 2009. Current-matched triple-junction solar cell reaching 41.1% conversion efficiency under concentrated sunlight. Applied Physics Letters 94, 223504.

Hein, M., Meusel, M., Baur, C., Dimroth, F., Lange, G., Siefer, G., Tibbits, T.N.D., Bett, A.W., Andreev, V.M. and Rumyantsev, V.D., 2001. Characterisation of a 25% high-efficiency fresnel lens module with GaInP/GaInAs dual-junction concentrator solar cells. In: Proceedings of the 17th European Photovoltaic Solar Energy Conference, pp. 496–499.

IEC 60904-3 – Ed.1, Photovoltaic Devices – Part 3: Measurement Principles for Terrestrial Photovoltaic (PV) Solar Devices with Reference Spectral Irradiance Data, 1989.

ISO 15387:2005, Space Systems – Single-Junction Solar Cells –Measurements and Calibration Procedures, 2005.

King, R.R., Law, D.C., Edmondson, K.M., Fetzer, C.M., Kinsey, G.S., Yoon, H., Sherif, R.A., Karam, N.H., 2007. 40% efficient metamorphic GaInP/GaInAs/Ge multijunction solar cells. Applied Physics Letters 90, 183516-1–183516-3.

Krishnan, P., Schüttauf, J.W.A., van der Werf, C.H.M., Houshyani Hassanzadeh, B., van Sark, W.G.J.H.M., Schropp, R.E.I., 2009. Response to simulated typical daily outdoor irradiation conditions of thin-film silicon-based triple-band-gap, triple-junction solar cells. Solar Energy Materials and Solar Cells 93, 691–697.

Kurtz, S.R., Faine, P., Olson, J.M., 1990. Modeling of two-junction, series-connected tandem solar cells using top-cell thickness as an adjustable parameter. Journal of Applied Physics 68, 1890–1895.

Létay, G., Baur, C., Bett, A.W., 2004. Theoretical investigations of III–V multi-junction concentrator cells under realistic spectral conditions. In: Proceedings of the 19th European Photovoltaic Solar Energy Conference, pp. 187–190.

Luque, A., Andreev, V.M., 2007. Concentrator Photovoltaics. Springer-Verlag, Heidelberg, Germany, p. 345.

McMahon, W.E., Emery, K.E., Friedman, D.J., Ottoson, L., Young, M.S., Ward, J.S., Kramer, C.M., Duda, A., Kurtz, S., 2008. Fill factor as a probe of current-matching for GaInP2/GaAs tandem cells in a concentrator system during outdoor operation. Progress in Photovoltaics: Research and Applications 16, 213–224.

Meusel, M., Adelhelm, R., Dimroth, F., Bett, A.W., Warta, W., 2002. Spectral mismatch correction and spectrometric characterization of monolithic III–V multi-junction solar cells. Progress in Photovoltaics: Research and Applications 10, 243–255.

Meusel, M., Baur, C., Siefer, G., Dimroth, F., Bett, A.W., Warta, W., 2006. Characterization of monolithic III–V multi-junction solar cells – challenges and application. Solar Energy Materials and Solar Cells 90, 3268–3275.

Minemoto, T., Fukushige, S., Takakura, H., 2009. Difference in the outdoor performance of bulk and thin-film silicon-based photovoltaic modules. Solar Energy Materials and Solar Cells 93, 1062–1065.

Minemoto, T., Toda, M., Nagae, S., Gotoh, M., Nakajima, A., Yamamoto, K., Takakura, H., Hamakawa, Y., 2007. Effect of spectral irradiance distribution on the outdoor performance of amorphous Si// thin-film crystalline Si stacked photovoltaic modules. Solar Energy Materials and Solar Cells 91, 120–122.

Ossenbrink, H., Münzer, K.A., 1992. The ESTI sensor – a new reference cell for monitoring of PV plant performance. In: 11th E.C. Photovoltaic Solar Energy Conference, pp. 333–336.

Rumyantsev, V.D., Sadchikov, N.A., Chalov, A.E., Ionova, E.A., Friedman, D.J., Glenn, G.S., 2006. Terrestrial concentrator PV modules based on GaInP/GaAs/Ge TJ cells and minilens panels. In: Proceedings of the 4th World Conference on Photovoltaic Energy Conversion, pp. 632–635.

Siefer, G., Abbott, P., Baur, C., Schlegl, T., Bett, A.W., 2005. Determination of the temperature coefficients of various III–V solar cells. In: Proceedings of the 20th European Photovoltaic Solar Energy Conference, pp. 495–498.

Siefer, G., Bett, A.W., 2005. Experimental comparison between the power outputs of FLATCON® modules and silicon flat plate modules. In: Proceedings of the 31st IEEE Photovoltaic Specialists Conference, pp. 643–646.

Siefer, G., Bett, A.W., Emery, K., 2004. One year outdoor evaluation of a FLATCON concentrator module. In: Proceedings of the 19th European Photovoltaic Solar Energy Conference, pp. 2078–2081.

Tsutsui, J., Kurokawa, K., 2008. Investigation to estimate the short circuit current by applying the solar spectrum. Progress in Photovoltaics: Research and Applications 16, 205–211.

van Sark, W.G.J.H.M., 2008. Simulating performance of solar cells with spectral downshifting layers. Thin Solid Films 516, 6808–6812.